
Log-Likelihood, Simpson’s Paradox, and the Detection of Machine-Generated Text

Tom Kempton*
Department of Mathematics
University of Manchester
thomas.kempton@manchester.ac.uk

Viktor Drobnyi
Risk and Security AI Lab
Visa Inc.
vdrobnyi@visa.com

Maeve Madigan
Risk and Security AI Lab
Visa Inc.
mmadigan@visa.com

Stuart Burrell
Risk and Security AI Lab
Visa Inc.
sburrell@visa.com

Abstract

The ability to reliably distinguish human-written text from that generated by large language models is of profound societal importance. The dominant approach to this problem exploits the likelihood hypothesis: that machine-generated text should appear more probable to a detector language model than human-written text. However, we demonstrate that the token-level signal distinguishing human and machine text is non-uniform across the hidden space of the detector model, and naively averaging likelihood-based token scores across regions with fundamentally different statistical structure, as most detectors do, causes a form of Simpson’s paradox: a strong local signal is destroyed by inappropriate aggregation. To correct for this, we introduce a learned local calibration step grounded in Bayesian decision theory. Rather than aggregating raw token scores, we first learn lightweight predictors of the score distributions conditioned on position in hidden space, and aggregate calibrated log-likelihood ratios instead. This single intervention dramatically and consistently improves detection performance across all baseline detectors and all datasets we consider. For example, our calibrated variant of Fast-DetectGPT improves AUROC from 0.63 to 0.85 on GPT-5.4 text, and a locally-calibrated DMAP detector we introduce achieves state-of-the-art performance across the board. That said, our central contribution is not a new detector, but a precise diagnosis of a significant cause of under-performance of existing detectors and a principled, modular remedy compatible with any token-averaging pipeline. This will serve as a foundation for the community to build upon, with natural avenues including richer distributional models, improved calibration strategies, and principled ensembling with hidden-space geometry signals via the full Bayes-optimal decision rule.

1 Introduction

The dominant approach to detecting machine-generated text rests on the *likelihood hypothesis*: text produced by a language model should appear more probable under a detector model than human-written text does, reflecting the tendency of generators to favor high-probability tokens. This signal has driven a generation of detectors [1, 2, 3, 4, 5, 6], and considerable effort has gone into extracting it as effectively as possible.

*Work completed while a consultant at the Risk and Security AI Lab, Visa Inc.

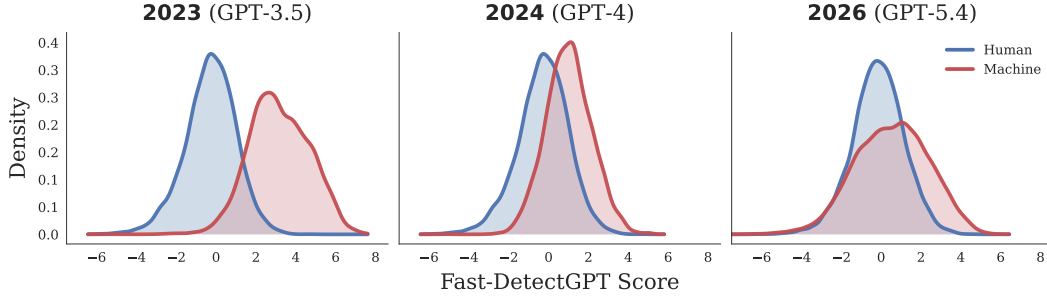


Figure 1: Performance of machine-generated text detectors appears to be degrading over time. These illustrative plots show Fast-DetectGPT scores for human-written and machine-generated text across three generations of instruction-tuned models: ChatGPT 3.5, GPT-4, and GPT-5.4. The separation between human and machine score distributions deteriorates markedly across generations, with AUROC falling from **0.96** on GPT-3.5 to **0.62** on GPT-5.4. We attribute this to the progressive mitigation of overconfidence in successive frontier models, which weakens the token-level signal that likelihood-based detectors rely upon. Extensive experiments in Section 5 and Appendix E provide further evidence of this degradation and highlight the need for effective new detection methodologies.

In practice, however, the likelihood hypothesis is weakening, with performance of likelihood-based detectors severely degrading as the models used to generate text improve; see Figure 1 and Appendix G. It was shown in [7] that the likelihood hypothesis fails as a method of detecting text generated by pure sampling from pretrained language models; when the likelihood hypothesis holds it is either because text has been generated using a sampling method such as top-k or temperature explicitly designed to avoid low-probability tokens, or because text has been generated by an overconfident instruction-tuned language model. The question of optimally detecting top-k and temperature-sampled text has been addressed in [8]; in this article we therefore focus on detecting text from instruction-tuned models, including modern closed-source frontier models such as GPT-5.4 [9], Gemini 3.1 Pro [10], and Claude Sonnet 4.6 [11]. In particular, our contribution is motivated by the following three recent advances in the literature, which we elaborate on further in Appendix A.

1. **Instruction-tuned models satisfy the likelihood hypothesis because of overconfidence.** It was argued in [7] that the reason the likelihood hypothesis continues to hold for instruction-tuned models is that the widely observed phenomenon of overconfidence caused by instruction tuning manifests as a token-level bias of instruction-tuned models towards tokens which a detector model finds likely.
2. **The degree of overconfidence varies across hidden space.** In [12] it was shown that overconfidence of instruction-tuned models does not present itself uniformly. In particular, it was shown that recalibrating models with temperature sampling is more effective when the chosen temperature varies as a function of the activation vector at the final hidden layer.
3. **Human and machine generated text occupy different parts of hidden space.** In [13] it was shown that one can distinguish human and machine text by examining activation vectors in hidden space of a detector model, with human and machine generated text typically occupying different regions of hidden space.

Together, these points suggest that we are at risk of a Simpson’s paradox, where aggregation across heterogeneous subgroups destroys local signal. A classic illustration of this exists in healthcare: Hospital A may have a higher survival rate than Hospital B for both mild and severe cases of a disease, yet Hospital B could have a higher overall survival rate, simply because it treats proportionally more mild cases with a lower base rate of mortality. We show in Figure 2 a similar phenomenon afflicts likelihood-based detectors: the token-level signal distinguishing human from machine text varies significantly across regions of hidden space, and naive averaging across those regions suppresses it because there are many regions dominating the aggregation where the signal is weaker or even reversed. Strong local signals exist, but current detectors fail to utilize them. Throughout this article we use the familiar term ‘Simpson’s paradox’ as shorthand for both true Simpson’s paradoxes and the broader case of failure of aggregation under heterogeneous conditional score distributions.

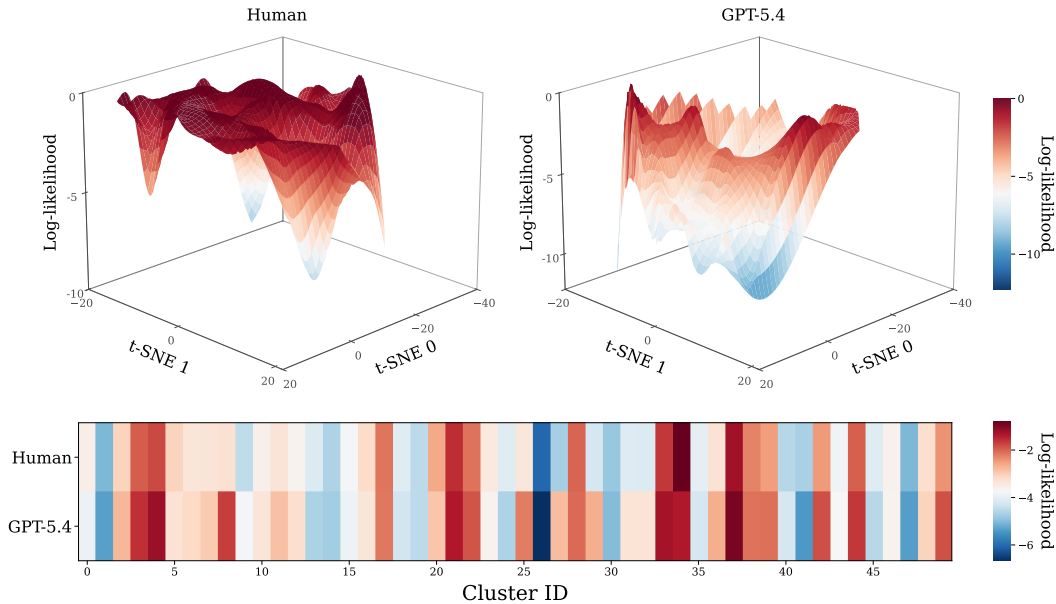


Figure 2: **Upper:** A single illustrative example showing how the geometry of the log-likelihood landscape can vary across hidden space and source (human vs. GPT-5.4). **Lower:** Systematic analysis of 4,000 texts from RAID [14]. While human text has lower average log-likelihood than GPT-5.4 (-3.22 vs. -3.05), this relationship reverses in some regions of hidden space, and variation *across* 50 k-means clusters exceeds variation *between* sources. This suggests that contextualizing token log-likelihood by hidden-space region provides a valuable untapped signal for detection. Further details on how to reproduce these plots are in Appendix D.

We validate this idea by inserting an extra step into the standard pipeline for detecting machine generated text. Instead of computing token-level scores, aggregating, and then thresholding, we add a learned local-calibration layer before aggregation, which prevents the problem of distortion due to different underlying statistics in different parts of hidden space; see Figure 3.

Our results strongly confirm that state-of-the-art detectors underperform due to the issues we describe, and that a learned local-calibration step dramatically improves performance across an array of state-of-the-art (SOTA) detectors. For example, we improve the AUROC of Fast-DetectGPT from 0.63 to 0.85 on GPT-5.4 generated texts by incorporating the local-calibration step. Our best performing approach, a locally-calibrated detector based on DMAP [7], outperforms all baselines.

Contributions

- **Demonstrate the weakening of the likelihood hypothesis.** We demonstrate that the performance of modern detectors is diminishing as overconfidence is mitigated in frontier models.
- **Identify a major cause of under-performance in modern detectors.** We demonstrate how a phenomenon resembling Simpson’s paradox leads to under-performance in modern detectors due to non-uniformity of token-level scores across hidden space.
- **Introduce learnable local calibration as a mitigation strategy.** Grounded in Bayesian decision theory, we derive a principled calibration step that learns local estimates of token-score distributions conditioned on position in hidden space, and aggregates calibrated log-likelihood ratios in place of raw token scores.
- **Validate that learned local calibrators significantly improve detection.** Across all baseline detectors and datasets considered, inserting a local calibration step before score aggregation yields substantial and consistent gains in AUROC, with locally-calibrated DMAP detector achieving state-of-the-art performance throughout.

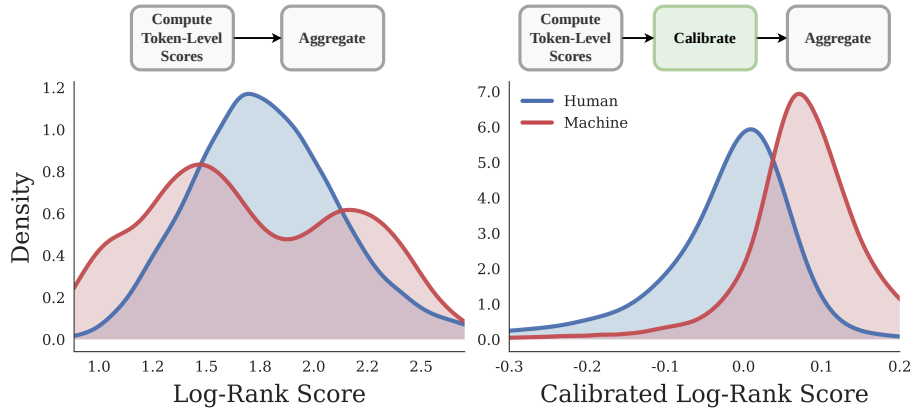


Figure 3: **Left:** Standard detection pipelines aggregate raw per-token scores directly, which may yield heavily overlapping distributions for human and modern GPT-5.4 text (AUROC 0.56). **Right:** Our pipeline inserts a local calibration step before aggregation, producing well-separated distributions (AUROC 0.91). The improvement reflects a Simpson’s paradox: token scores have heterogeneous local statistics across hidden-space regions, and naive aggregation obscures the underlying signal.

We emphasize that our primary goal is not to propose a new detector, but to isolate and correct a fundamental flaw in how existing detectors aggregate information. The local calibration step we introduce is deliberately lightweight, theoretically grounded, and architecture-agnostic: it can be inserted into any token-averaging detection pipeline with minimal overhead. We intentionally avoid extensive hyperparameter tuning or dataset-specific optimization, precisely because we want to demonstrate that the gains arise from correcting a statistical pathology rather than from over-engineering to a particular benchmark. By identifying a root cause of detector under-performance and providing a modular remedy, we offer the community a foundation to build upon with further optimization.

2 Related Work

Likelihood-based detection. The most widely used signal in machine-generated text detectors is per-token log-likelihood [1], which takes a text $w_1 \cdots w_n$ and a detector language model p and computes $\frac{1}{n} \sum_{i=1}^n \log(p(w_i | w_1 \cdots w_{i-1}))$. Per-token log-rank is similar, replacing likelihood with the rank of token w_i in the vocabulary ordered by decreasing probability under $p(\cdot | w_1 \cdots w_{i-1})$. Both exploit the likelihood hypothesis: machine-generated text should sit higher in the probability distribution of a detector model than human-written text.

Contextualisation of token-level scores. A natural limitation of raw likelihood and log-rank scores is that they vary substantially across writing styles and domains; the next token in a piece of poetry is inherently less predictable than in a chemistry textbook. DetectGPT [2] addressed this by subtracting from the log-likelihood of a text the expected log-likelihood of alternative phrasings of the same content. Fast-DetectGPT, DetectLLM, Binoculars, and DMAP all build on this contextualisation idea [3, 5, 4, 7]. While DMAP was not originally proposed as a detector of machine-generated text, it presents a contextualised generalisation of log-rank with well-understood statistical properties that makes it a natural fit for our framework; we adapt it to produce a detector in Appendix C.

Complementary approaches. Methods that exploit patterns in the log-likelihood sequence [15, 16], statistical signatures of specific decoding strategies [8], and geometric differences between human and machine text in embedding space [17, 13] offer signals that are largely orthogonal to the likelihood signal, making them natural candidates for ensembling with likelihood-based methods.

Zero-shot versus supervised detection. The detectors above are zero-shot: no labelled training data is required to produce a score, though a labelled set is needed to learn a decision threshold. Supervised approaches treat detection as a classification task directly. DALD [6] occupies a middle

ground, fine-tuning the detector model to better match the statistics of a target generator before applying the Fast-DetectGPT scoring procedure. Our approach is closest in spirit to DALD, but rather than fine-tuning the detector model to achieve white-box performance we calibrate the interpretation of token-level scores.

3 Calibrating Score Functions with Bayesian Decision Theory

Suppose we have a text $w_1 \cdots w_n$ which we wish to classify as human-written or machine-generated. Let $x = w_1 \cdots w_n$ and $x_i = w_i | w_1 \cdots w_{i-1}$.

The standard pipeline. Token-level score functions work as follows. The text is run through a detector language model and each token is assigned a score $g(x_i)$, as described in Section 4.1. These scores are aggregated to produce a text-level score $\frac{1}{n} \sum_{i=1}^n g(x_i)$, which is then thresholded against a value learned from a labelled set of human-written and machine-generated texts.

Naive aggregation. This aggregation of g is optimal only if the distribution of token scores $g(x_i)$ is independent of any other information available to us. As argued in the introduction, this assumption fails: the statistical distribution of token-level scores varies significantly across regions of hidden space, and aggregating naively across these regions suppresses the local signal. This is precisely the phenomenon identified in Section 1 where inappropriate averaging of heterogeneous local score distributions weakens the global signal.

To see this more formally, suppose the only information available about a text is its aggregate score $\alpha = \frac{1}{n} \sum_{i=1}^n g(x_i)$. Let H and M denote the hypothesis that the text is human-written or machine-generated respectively. The Neyman-Pearson lemma states that the optimal test thresholds the log-likelihood ratio

$$\Lambda_1(\alpha) = \log \left(\frac{\mathbb{P}(\text{score} = \alpha | H)}{\mathbb{P}(\text{score} = \alpha | M)} \right).$$

Given the reasonably smooth score distributions shown in Figure 1, thresholding directly on α is a reasonable proxy for this. However, the aggregate score is not the only information available to us, and exploiting additional information can substantially improve detection.

The Bayes-optimal decision rule. Let $Z(x_i)$ denote additional features extracted at the token level, specifically a low-dimensional projection of the activation vector at the final hidden layer of the detector model, together with properties of the next-token probability distribution $p(\cdot | w_1 \cdots w_{i-1})$. The precise construction of $Z(x_i)$ is described in Section 4.

Given token-level scores $g(x_i)$ and features $Z(x_i)$, the Bayes-optimal decision rule is to threshold the log-likelihood ratio of the full observed data,

$$\Lambda_2 = \log \left(\frac{\mathbb{P}(\{g(x_i), Z(x_i)\}_{i=1}^n | H)}{\mathbb{P}(\{g(x_i), Z(x_i)\}_{i=1}^n | M)} \right).$$

Learning the full sequence distributions $\mathbb{P}(\cdot | H)$ and $\mathbb{P}(\cdot | M)$ is intractable. Assuming instead that token-level scores are conditionally independent from one another given features and hidden space features are conditionally independent across tokens, the Bayes-optimal decision rule decomposes as

$$\begin{aligned} \Lambda_3 &= \sum_{i=1}^n \log \left(\frac{\mathbb{P}(g(x_i), Z(x_i) | H)}{\mathbb{P}(g(x_i), Z(x_i) | M)} \right) \\ &= \sum_{i=1}^n \left(\log \left(\frac{\mathbb{P}(g(x_i) | Z(x_i), H)}{\mathbb{P}(g(x_i) | Z(x_i), M)} \right) + \log \left(\frac{\mathbb{P}(Z(x_i) | H)}{\mathbb{P}(Z(x_i) | M)} \right) \right). \end{aligned} \quad (1)$$

Note that these conditional independence assumptions are unlikely to hold precisely, and there is likely significant room for improvement by relaxing them; see Section 6.

Interpreting the decomposition. The two terms in Equation 1 capture complementary sources of signal. The first term is a locally-calibrated likelihood ratio: it asks how probable the token score $g(x_i)$ is, given the local context $Z(x_i)$ and the hypothesis that the text is human-written or

machine-generated. This is the signal that naive aggregation suppresses. The second term captures how much the position of the token in hidden space itself discriminates between human and machine text, independently of the score; this is the principle underlying the detector of [13].

Our calibrated score. The purpose of this paper is to demonstrate the power of calibrating existing score functions using local information $Z(x_i)$, rather than to ensemble likelihood-based scores with hidden-space geometry signals. Our calibration step therefore uses only the first term of equation (1). For a fixed generator model M , we learn plug-in estimates of $\mathbb{P}(g(x_i) | Z(x_i), H)$ and $\mathbb{P}(g(x_i) | Z(x_i), M)$ and compute their log-ratio, returning the calibrated score

$$\Lambda_4 = \sum_{i=1}^n \log \left(\frac{\mathbb{P}(g(x_i) | Z(x_i), H)}{\mathbb{P}(g(x_i) | Z(x_i), M)} \right).$$

The implementation of these plug-in estimators is described in Section 4.

4 Implementing Local Calibration

In this section we describe our implementation of the local calibration step, and in particular how we learn plug-in estimates for the probabilities $\mathbb{P}(g(x_i)|Z(x_i), H)$ and $\mathbb{P}(g(x_i)|Z(x_i), M)$. In deployment, careful thought should be given to the design of the calibration step, based on the specific score function whose performance one seeks to optimise, the nature of the texts one wishes to analyse, and the desired balance between false positives and false negatives. For example, one may wish to place upper and lower bounds on the contribution of any single token so that the aggregate score is not dominated by a handful of extreme values.

Our goal here is to demonstrate to the community that calibration works, and that it dramatically improves the performance of all baseline detectors we consider. We therefore deliberately adopt a naive implementation, learning a local Gaussian predictor of each score function at different positions in hidden space, without any hyperparameter tuning. This already yields dramatic improvements as we shall see in Section 5, but leaves substantial room for further performance gains through more careful design choices, which we discuss in Section 6.

4.1 Baseline Score Functions

Our focus is on extracting signal based on the likelihood hypothesis. We use as baselines the most successful approaches in this family: Fast-DetectGPT [3], Binoculars [4], NPR [5], per-token log-surprisal, and per-token log-rank [1]. Approaches that use the likelihood signal in complementary ways, for example by examining local fluctuations or differences between the first and second halves of a text, are orthogonal to our investigation and are not included as baselines.

For our calibration step to apply, a detector must operate by averaging a token-level score function g over the tokens in a text. Per-token log-likelihood sets

$$g(w_i|w_1 \cdots w_{i-1}) = \log(p(w_i|w_1 \cdots w_{i-1}))$$

and computes $\sum_{i=1}^n g(w_i|w_1 \cdots w_{i-1})$. Per-token log-rank sets

$$g(w_i|w_1 \cdots w_{i-1}) = \log(r(w_i|w_1 \cdots w_{i-1})),$$

where r denotes the rank of the token under p .

NPR, Binoculars, and Fast-DetectGPT are not direct averages of token-level scores. For example, Fast-DetectGPT sums log-likelihood and entropy over a text but then normalises by the variance of the scores rather than the token count. For these baselines we use the true function as the reported baseline score, but train our locally-calibrated variant using a token-level approximation. Full details of each baseline and its token-level counterpart are given in Appendix B.

4.2 Learning Local Score Distributions

Given a sequence of tokens $w_1 \cdots w_{i-1}$ as context, we define the *hidden vector* as the activation vector at the final hidden layer of the detector model when processing that context. We first perform PCA on the hidden vectors to identify d principal directions in hidden space (in our experiments

Table 1: Token-level scoring functions are substantially improved by adding a local calibration step. This contextualizes the score based on the location in hidden space. Confidence intervals for all values are provided by the companion Table 4 in Appendix E.

Method	Modern RAID			Peer-Review		
	GPT-5.4	Gemini	Claude	GPT-4o	Gemini	Claude
Baseline Log-Surprisal	0.562	0.506	0.631	0.635	0.559	0.514
Calibrated Log-Surprisal	0.918	0.893	0.937	0.954	0.969	0.990
Baseline Log-Rank	0.544	0.468	0.608	0.602	0.527	0.479
Calibrated Log-Rank	0.856	0.781	0.869	0.826	0.835	0.910
Baseline Token-NPR	0.603	0.686	0.768	0.616	0.584	0.537
Calibrated Token-NPR	0.834	0.749	0.856	0.809	0.813	0.900
Baseline Token-FastDetectGPT	0.628	0.734	0.800	0.640	0.607	0.545
Calibrated Token-FastDetectGPT	0.854	0.805	0.868	0.862	0.861	0.932
Baseline DMAP	0.689	0.779	0.805	0.834	0.952	0.861
Calibrated DMAP	0.939	0.937	0.961	0.973	0.979	0.994

$d = 25$). For each context in the training set, the feature vector $Z(x_i)$ is then formed by concatenating this d -dimensional projection of the hidden vector with the model probabilities of the top- k (we set $k = 5$ in our experiments) candidate tokens, yielding a $(d + k)$ -dimensional feature vector. We then train, for each generator model including human, a local DMAP predictor and local Gaussian predictors of other score functions using a simple two layer MLP as described in Appendix D.

Computing the calibrated score. Given a context, a true next token, and plug-in estimators for human and machine distributions, we compute Λ_4 by subtracting the log-loss of the human predictor from that of the machine predictor, token by token, and summing over the text. This yields the locally-calibrated score defined in Section 3.

5 Experiments

5.1 Experimental Setup

We evaluate on three datasets spanning different domains, generators, and time periods. Classic RAID [14] pairs human-written texts across eight domains with machine-generated counterparts from GPT-3.5 and GPT-4, generated via pure sampling without evasion attacks. Modern RAID extends this to current frontier models by regenerating responses following the original prompt templates using GPT-5.4 [9], Gemini 3.1 Pro [10], and Claude Sonnet 4.6 [11] with default sampling settings. Finally, the Peer-Review benchmark [18] contains reviews of ICLR and NeurIPS submissions (2021–2022) generated by GPT-4o, Claude Sonnet 3.5, and Gemini Pro 1.5.

We use OPT-125M as the detector model in all experiments except for the Binoculars baseline, which uses the Falcon-3-7B scorer–observer pair following [4]. For each dataset and generator, we hold out a fixed subset for training local predictors, with the remainder used for evaluation. We report AUROC as our primary metric. Our main results use only the first 200 tokens of each text to facilitate direct and fair comparison; additional experimental details are provided in Appendix D.

5.2 Discussion of Results

In Table 1 we compare token-level scorers to their calibrated counterparts. In Table 2 we compare the calibrated DMAP detector to state-of-the-art detection baselines. We report AUROC here, while Tables 6, 7 and 8 in Appendix E contain the same results but also report 95% confidence intervals and true-positive rates at false positive rates 0.1% and 1%.

Local calibration consistently improves detection. Table 1 compares baseline token-level scorers to their locally-calibrated counterparts. The improvement is substantial and universal: calibration

Table 2: Calibrated DMAP outperforms state-of-the-art baselines. Confidence intervals for all values are provided by the companion Table 5 in Appendix E.

Method	Modern RAID			Peer-Review		
	GPT-5.4	Gemini	Claude	GPT-4o	Gemini	Claude
NPR	0.526	0.503	0.554	0.600	0.582	0.496
Binoculars	0.692	0.537	0.628	0.289	0.626	0.508
Fast-DetectGPT	0.629	0.733	0.799	0.640	0.606	0.543
DALD	0.894	0.957	0.943	0.852	0.865	0.965
Calibrated DMAP	0.939	0.937	0.961	0.973	0.979	0.994

improves AUROC for every scorer, every generator, and every dataset: a total of 30 out of 30 comparisons, even though our implementation of calibration is deliberately naive. The gains are particularly pronounced where baselines struggle most: on GPT-5.4, calibrated log-surprisal improves from 0.562 to 0.918, and calibrated DMAP improves from 0.689 to 0.939. Even strong baselines benefit; calibrating Token-FastDetectGPT on Claude (Peer-Review) raises AUROC from 0.545 to 0.932. These consistent gains across diverse settings confirm that the uncalibrated aggregation of token-scores is a fundamental and pervasive source of signal loss, not confined to any particular detector or dataset. We also run an analysis of the robustness of our calibrated detectors to domain shift, results in Table 10 show the uplift in performance from calibration is less strong under domain shift but still comfortably outperforms zero-shot baselines.

Calibrated DMAP achieves state-of-the-art performance. Table 2 compares our calibrated DMAP detector against leading baselines. Calibrated DMAP achieves the highest AUROC in 5 of 6 settings, and is within 0.02 of the best method (DALD) in the remaining case. The margin over zero-shot methods is substantial: on GPT-5.4, calibrated DMAP (0.939) outperforms Fast-DetectGPT (0.629) by over 0.30 AUROC. Appendix H shows that even stronger results are possible via some simple methods to improve Calibrated DMAP. For example, increasing the hidden dimension of the calibration head, increasing the number of bins in DMAP and training for longer allows one to increase the AUROC of calibrated DMAP on GPT-5.4 texts reported in Table 2 from 0.939 to 0.968, further increasing our performance advantage over baselines. Appendix E also reports the effectiveness of our calibrated detectors in detecting texts where the precise generating language model is unknown. These results highlight the importance of considering how best to ensemble scores from multiple detectors, each of which target a particular generator model. Our results show that even our simple approach is competitive, and in particular, zero-shot alternatives fall far behind Calibrated DMAP and DALD in this setting.

6 Future Directions

Throughout this paper we have deliberately adopted a simple experimental approach, restricting ourselves to signal derived from the likelihood hypothesis and avoiding hyperparameter tuning. This conservative stance is a feature rather than a shortcoming: our goal is to demonstrate that even a naive calibration step yields dramatic performance improvements. We identify four directions where targeted effort would yield the most significant further gains.

Richer distributional models. The most significant limitation of our current implementation is the use of simple Gaussians to model $\mathbb{P}(g(x_i)|Z(x_i), H)$ and $\mathbb{P}(g(x_i)|Z(x_i), M)$. These are clearly suboptimal; log-rank, for example, takes non-negative discrete values with the most common value being 0, making Gaussian approximations a poor fit. The weakness of the Gaussian assumption for log-likelihood is examined in Appendix F. Replacing these with more expressive density estimators, such as normalizing flows or mixture models, would be a natural first step.

Robustness to imperfect calibration. Bayes-optimal decision theory assumes that the class-conditional distributions are known exactly. In practice, our plug-in estimators are imperfect, and the consequences of this imperfection depend on the relative cost of false positives and false negatives, the statistics of the dataset, and the properties of the score function. Principled interventions, such as

capping the per-token contribution to the aggregate score to limit the influence of poorly estimated tails, would improve robustness and deserve systematic investigation.

Incorporating hidden-space geometry. In deriving Λ_4 we deliberately set aside the second term of equation (1), which captures how much the position of a token in hidden space itself discriminates between human and machine text. Given the effectiveness of [13], we expect that learning plug-in estimates of $\mathbb{P}(Z(x_i)|H)$ and $\mathbb{P}(Z(x_i)|M)$ and incorporating them into the decision rule would yield substantial further gains, effectively ensembling our calibrated likelihood signal with a hidden-space geometry signal in a principled, Bayes-optimal manner.

Relaxing conditional independence. In moving from Λ_2 to Λ_3 we assume that token-level scores are conditionally independent given features. This assumption is known to fail: several detectors are explicitly built around the sequential dependencies in the log-likelihood sequence [15, 16]. With sufficient training data, learning the full conditional distributions in Λ_2 directly, rather than factorising over tokens, would be expected to yield further improvements.

7 Conclusion

The performance of likelihood-based detectors of machine-generated text is degrading rapidly as the overconfidence of instruction-tuned frontier models is reduced. For example, we see Fast-DetectGPT, representative of the state of the art, achieves an AUROC of 0.96 on GPT-3.5 text, 0.79 on GPT-4 text, and 0.63 on GPT-5.4 text.

We have identified a significant and previously unrecognized cause: naive aggregation of token-level scores across regions of hidden space with fundamentally different statistical structure constitutes a form of Simpson’s paradox, suppressing a local signal that remains strong. The fix is principled and modular. By inserting a learned local calibration step between token scoring and score aggregation, grounded in Bayesian decision theory, we recover dramatic performance improvements across every baseline detector and dataset we consider. Our locally-calibrated Fast-DetectGPT improves from 0.63 to 0.85 AUROC on GPT-5.4 text; our locally-calibrated DMAP detector achieves state-of-the-art performance throughout. Critically, these gains are achieved with a deliberately naive implementation, leaving substantial further headroom identified in Section 6.

The central contribution of this paper is not a new detector. It is a precise diagnosis of a way that existing detectors underperform, a Bayes-optimal framework for correcting this, and a demonstration that even the simplest instantiation of that framework yields dramatic gains. As frontier models continue to close the gap with human writing, we hope this work provides the community with both the conceptual tools and a practical foundation to meet the challenge.

8 Limitations and Societal Impact

Our calibration step requires training separate predictors for each generator one wishes to detect, unlike zero-shot alternatives which purport to generalize to arbitrary sources. We offer two partial defenses. First, claims that zero-shot methods generalize to arbitrary generators are overstated: it was shown in [7] that results supporting such claims were based on flawed evaluation data, and that DetectGPT, Fast-DetectGPT, and Binoculars all perform below chance when detecting text generated by pure sampling from non-instruction-tuned models. Second, our method outperforms all zero-shot baselines even in the multi-generator setting (Table 9). Nevertheless, deploying our method in practice requires committing to a set of target generators at training time. A second limitation is the absence of a large public dataset spanning several years of frontier model development; no such resource currently exists, and direct comparisons between results across our two datasets should be interpreted with care given differences in domain, prompting strategy, and text length. Finally, all experiments are conducted on English-language texts, and generalization to other languages remains an open question.

We believe that, appropriately used, detectors of machine generated text are a net positive for society. That said, we emphasize care must be taken in deployment, particularly with regard to ensuring that different demographics are not unfairly penalized and in understanding the possibility for false

positives. Therefore, in practice, the continual monitoring of any detection system is a critical safeguard.

References

- [1] Sebastian Gehrmann, Hendrik Strobelt, and Alexander M Rush. GLTR: Statistical Detection and Visualization of Generated Text. In *Proceedings of the 57th Annual Meeting of the Association for Computational Linguistics: System Demonstrations*, pages 111–116, 2019.
- [2] Eric Mitchell, Yoonho Lee, Alexander Khazatsky, Christopher D Manning, and Chelsea Finn. DetectGPT: Zero-Shot Machine-Generated Text Detection using Probability Curvature. In *International Conference on Machine Learning*, pages 24950–24962. PMLR, 2023.
- [3] Guangsheng Bao, Yanbin Zhao, Zhiyang Teng, Linyi Yang, and Yue Zhang. Fast-DetectGPT: Efficient Zero-Shot Detection of Machine-Generated Text via Conditional Probability Curvature. In *The Twelfth International Conference on Learning Representations*, 2023.
- [4] Abhimanyu Hans, Avi Schwarzschild, Valeriia Cherepanova, Hamid Kazemi, Aniruddha Saha, Micah Goldblum, Jonas Geiping, and Tom Goldstein. Spotting LLMs With Binoculars: Zero-Shot Detection of Machine-Generated Text. In *Proceedings of the 41st International Conference on Machine Learning*, pages 17519–17537, 2024.
- [5] Jinyan Su, Terry Zhuo, Di Wang, and Preslav Nakov. DetectLLM: Leveraging Log Rank Information for Zero-Shot Detection of Machine-Generated Text. In *Findings of the Association for Computational Linguistics: EMNLP 2023*, pages 12395–12412, 2023.
- [6] Cong Zeng, Shengkun Tang, Xianjun Yang, Yuanzhou Chen, Yiyu Sun, Zhiqiang Xu, Yao Li, Haifeng Chen, Wei Cheng, and Dongkuan Xu. DALD: Improving Logits-based Detector without Logits from Black-box LLMs. *Advances in Neural Information Processing Systems*, 37:54947–54973, 2024.
- [7] Tom Kempton, Julia Rozanova, Parameswaran Kamalaruban, Maeve Madigan, Karolina Wresilo, Yoann Launay, David Sutton, and Stuart Burrell. DMAP: A Distribution Map for Text. In *The Fourteenth International Conference on Learning Representations*, 2026.
- [8] Tom Kempton, Stuart Burrell, and Connor J Cheverall. TempTest: Local Normalization Distortion and the Detection of Machine-generated Text. In *International Conference on Artificial Intelligence and Statistics*, pages 1972–1980. PMLR, 2025.
- [9] OpenAI. GPT-5 system card. Technical report, OpenAI, August 2025. arXiv:2601.03267.
- [10] Google DeepMind. Gemini 3.1 Pro Model Card. Technical report, Google DeepMind, February 2026.
- [11] Anthropic. Claude Sonnet 4.6 System Card. Technical report, Anthropic, February 2026.
- [12] Johnathan Xie, Annie S Chen, Yoonho Lee, Eric Mitchell, and Chelsea Finn. Calibrating Language Models with Adaptive Temperature Scaling. In *Proceedings of the 2024 Conference on Empirical Methods in Natural Language Processing*, pages 18128–18138, 2024.
- [13] Xin Chen, Junchao Wu, Shu Yang, Runzhe Zhan, Zeyu Wu, Ziyang Luo, Di Wang, Min Yang, Lidia S Chao, and Derek F Wong. ReprGuard: Detecting LLM-Generated Text by Revealing Hidden Representation Patterns. *Transactions of the Association for Computational Linguistics*, 13:1812–1831, 2025.
- [14] Liam Dugan, Alyssa Hwang, Filip Trhlík, Andrew Zhu, Josh Magnus Ludan, Hainiu Xu, Daphne Ippolito, and Chris Callison-Burch. RAID: A Shared Benchmark for Robust Evaluation of Machine-Generated Text Detectors. In *Proceedings of the 62nd Annual Meeting of the Association for Computational Linguistics (Volume 1: Long Papers)*, pages 12463–12492, 2024.
- [15] Ke Sun, Guangsheng Bao, Han Cui, and Yue Zhang. When AI Settles Down: Late-Stage Stability as a Signature of AI-Generated Text Detection. *arXiv preprint arXiv:2601.04833*, 2026.

- [16] Haitong Luo, Weiyao Zhang, Suhang Wang, Wenji Zou, Chungang Lin, Xuying Meng, and Yujun Zhang. SpecDetect: Simple, Fast, and Training-Free Detection of LLM-Generated Text via Spectral Analysis. In *Proceedings of the AAAI Conference on Artificial Intelligence*, volume 40, pages 32356–32364, 2026.
- [17] Eduard Tulchinskii, Kristian Kuznetsov, Laida Kushnareva, Daniil Cherniavskii, Sergey Nikolenko, Evgeny Burnaev, Serguei Barannikov, and Irina Piontkovskaya. Intrinsic Dimension Estimation for Robust Detection of AI-Generated Texts. *Advances in Neural Information Processing Systems*, 36, 2024.
- [18] Sungduk Yu, Man Luo, Avinash Madasu, Vasudev Lal, and Phillip Howard. Is Your Paper Being Reviewed by an LLM? Benchmarking AI Text Detection in Peer Review. In *The Fourteenth International Conference on Learning Representations*, 2026.
- [19] Laurens van der Maaten and Geoffrey Hinton. Visualizing data using t-sne. *Journal of Machine Learning Research*, 9(86):2579–2605, 2008.

A Why one should expect naive token-score aggregation to underperform

In the introduction we made three claims motivating Simpson’s paradox based on previous results in the literature. In this section we expand on those claims, give more detail about how they are supported by the literature, and give evidence from our experiments to support them directly.

A.1 Instruction-tuned models satisfy the likelihood hypothesis because of overconfidence

The article [7] gives a method of viewing how a text sits in the next-token probability distributions of a language model. DMAP plots allow one to see how different parts of the detector model next-token probability distribution are over or under represented in the text, compared to the predictions of the detector model. Figures 2 and 8 of [7] show that instruction-tuned models such as ChatGPT or Mistral-7B Instruct systematically over-sample tokens which the detector model finds likely, leading to a situation where likelihood-based detectors of machine-generated text are effective. By contrast, pretrained language models such as Mistral-7B oversample tokens which the detector model finds unlikely, leading to a situation where likelihood-based detectors of machine-generated text perform worse than a coin-toss. See in particular Table 1 of [7], where it was shown that DetectGPT, Fast-DetectGPT and Binoculars all have AUROC well below 0.5 for detecting texts made by pure-sampling from Llama-3.1-8B, Mistral-7B or Qwen3-8B. This was linked to the phenomenon of over-confidence in instruction-tuned models.

A.2 Overconfidence Varies across Hidden Space

In the introduction we justified the claim that the phenomenon of token-level overconfidence is not uniform across hidden space by appealing to the work [12], where it was shown that temperature based recalibration of instruction-tuned models works best when the temperature used for recalibrating each token generation step varies with the position in hidden space.

Here we provide direct evidence. We use the training set from Modern RAID with human and GPT-5.4 completions and use k-means clustering to divide our PCA projection of hidden space into fifty regions. We then plot over the test set the average value of log-likelihood of GPT-5.4 generated tokens and human-generated tokens for each region of hidden space. Results are shown in Figure 2.

We see that, while it is generally true GPT-5.4-generated tokens have higher log-likelihood than human written tokens, the values vary dramatically between different regions of hidden space, and some regions even have GPT-5.4 tokens having lower log-likelihood than human written tokens.

A.3 Human and Machine-Generated Text Occupy Different Parts of Hidden Space

We previously justified the idea that machine and human text occupy different regions of hidden space by noting the work [13] which used this idea to build a detector of machine-generated text. To confirm the hypothesis, we analyse the distributions of human and machine-generated contexts among the fifty clusters of hidden space generated for our previous experiment. We show the proportions of GPT-5.4 and human generated text in each cluster in Table 3.

Table 3: We run k-means clustering to partition hidden space into 50 regions. We show statistics for the 10 largest clusters. There are clear differences in both the proportion of each cluster corresponding to human and GPT5 tokens and the mean values of the log-likelihood of human and GPT5 generated tokens within each cluster. Differences between clusters are stronger than differences between GPT5 and human text.

Cluster ID	Tokens in Cluster	Prop. Human	Prop. GPT-5	Mean log p (Human)	Mean log p (GPT-5)
4	120,057	0.511	0.489	-1.778	-1.182
21	76,984	0.514	0.486	-1.555	-1.386
2	57,594	0.557	0.443	-3.080	-2.756
5	54,897	0.362	0.638	-3.083	-3.306
11	46,805	0.440	0.560	-3.353	-2.877
49	44,854	0.449	0.551	-2.417	-1.857
15	44,465	0.135	0.865	-3.792	-3.874
13	43,404	0.443	0.557	-4.129	-4.652
38	43,183	0.286	0.714	-2.270	-2.132
31	42,547	0.445	0.555	-4.112	-3.324

B Scoring Functions

Our experiments involve calibrated versions of five detection methods: DMAP, log-likelihood, log-rank, Fast-DetectGPT and NPR. The first three of these are true token-level scorers, which score a text by aggregating scores of tokens. DMAP is described in Section C. Log-likelihood computes $\frac{1}{N} \sum_{i=1}^N \log(p(w_i|w_1 \cdots w_{i-1}))$ where p is the model probability from our observer model. Log-rank instead aggregates $r(w_i|w_1 \cdots w_{i-1})$ where this function gives the position of w_i in the list of possible choices of next token ordered by decreasing model probability $p(\cdot|w_1 \cdots w_{i-1})$. Fast-DetectGPT and NPR are discussed below.

B.1 Fast-DetectGPT

Fast-DetectGPT and NPR are not aggregates of token level scores, and so we need to adapt them in order to fit them into our pipeline. Fast-DetectGPT works by first computing a token score

$$g(w_i|w_1 \cdots w_{i-1}) = \log(p(w_i|w_1 \cdots w_{i-1})) - \sum_{v \in V} p(v|w_1 \cdots w_{i-1}) \log(p(v|w_1 \cdots w_{i-1})).$$

The second term here is the entropy of the next-token probability distribution, or equivalently, the expected value of the negative log-likelihood of a token randomly chosen according to the detector model. It gives a clever way of contextualising the log-likelihood of the true next token in the text in terms of the log-likelihood of alternatives. However, the final Fast-DetectGPT score is not obtained by aggregating token level scores, instead one divides by the standard deviation of the token level scores. This is problematic, see Section J. We recover a token-level approximation to Fast-DetectGPT by computing

$$FD_{\text{tok}}(w_1 \cdots w_n) := \frac{1}{n} \sum_{i=1}^n \left(\log(p(w_i|w_1 \cdots w_{i-1})) - \sum_{v \in V} p(v|w_1 \cdots w_{i-1}) \log(p(v|w_1 \cdots w_{i-1})) \right).$$

Our token-level approximation to the true Fast-DetectGPT usually underperforms the true version, but after calibration our token-level approximation greatly outperforms the baseline.

B.2 NPR

NPR works as follows. Given a text $w = w_1 \cdots w_n$ one first generates k perturbations of the original text using the T5 mask-filling model, call these $\underline{w}^{(j)}$. For the original text and for each of the perturbations compute the per-token log-rank. Finally output

$$NPR(w) = \frac{\text{per-token log-rank}(w)}{\frac{1}{k} \sum_{j=1}^k \text{per-token log-rank}(\underline{w}^{(j)})}.$$

This is not an aggregate of token-level scores. We approximate the NPR idea as follows. Instead of dividing by expected log-rank of perturbations of the whole text, we subtract the expected log-rank of perturbations of each token, following the method of Fast-DetectGPT. That is, we compute token-level scores

$$g(w_i|w_1 \cdots w_{i-1}) = \log(r(w_i|w_1 \cdots w_{i-1})) - \sum_{v \in V} p(v|w_1 \cdots w_{i-1}) \log r(v|w_1 \cdots w_{i-1}).$$

We then compute

$$\begin{aligned} & NPR_{\text{tok}}(w_1 \cdots w_n) \\ &= \frac{1}{n} \sum_{i=1}^n \left(\log(r(w_i|w_1 \cdots w_{i-1})) - \sum_{v \in V} p(v|w_1 \cdots w_{i-1}) \log r(v|w_1 \cdots w_{i-1}) \right). \end{aligned}$$

This is intended to approximate the idea of NPR with a token-level scorer amenable to our calibration methods. As with Fast-DetectGPT, we see that replacing NPR with its token-level approximation does not always increase the score, but after calibration the token-level approximation is much better than the original NPR baseline.

C Adapting DMAP to Detect Machine-Generated Text

DMAP [7] was introduced as a variant of log-likelihood and log-rank with more predictable statistical properties and greater robustness to extremes. We adapt it here to produce a detector of machine-generated text.

Recall that given a text $w_1 \cdots w_n$ and a language model p , the rank of token w_i is its position in the vocabulary ordered by decreasing probability under $p(\cdot|w_1 \cdots w_{i-1})$, with the most probable token having rank 1. This notion of position is blind to the actual probabilities involved. DMAP instead defines a_i as the total probability mass assigned by p to all tokens it considers more likely than w_i . The value a_i lies in $[0, 1]$ and equals 0 whenever w_i is the most probable next token. Setting $b_i := a_i + p(w_i|w_1 \cdots w_{i-1})$, the interval $[a_i, b_i] \subset [0, 1]$ has length equal to the probability of w_i and its position within $[0, 1]$ reflects how far down the next-token distribution w_i sits. Formal statistical properties of DMAP are established in [7].

Given a partition of $[0, 1]$ into k bins, one can measure what proportion of $[a_i, b_i]$ lies in each bin. DMAP sums these proportions over $i \in \{1, \dots, n\}$ to produce a histogram.

In our adaptation, we are particularly interested in the extent to which a text contains tokens drawn from the tail of the probability distribution. We partition $[0, 1]$ into six bins: $[0, 0.5]$, $[0.5, 0.75]$, $[0.75, 0.9]$, $[0.9, 0.95]$, $[0.95, 0.975]$, and $[0.975, 1]$. The resulting histogram is normalised by dividing each bin value by the bin width, so that text generated by pure sampling from p produces a flat histogram. The choice of partition can be considered a hyperparameter, and we expect tuning to further increase performance.

To score a test text, we first compute DMAP histograms over a training set of human-written and machine-generated texts, yielding representative length-six vectors q_{human} and q_{model} . For each token w_i in the test text, we compute the proportions $q_i = (q_{i,1}, \dots, q_{i,6})$ of the interval $[a_i, b_i]$ falling in each bin, and measure the cross-entropy of q_i against q_{human} and q_{model} respectively. Subtracting one from the other yields a humanness score for the token, which we then aggregate over the text. This is our Global DMAP detector.

As with other detectors, we see a substantial uplift to performance when we calibrate token level scores by incorporating information about where a context sits in hidden space, as described in Section 4.

D Experimental Details

We split datasets into train/test, with all texts corresponding to the same prompt ending up in the same split. For each dataset we take approximately 2000 texts from each generator (including human generated text) for training and keep the remainder for test. The same training texts are used to run the PCA and train the local calibrators.

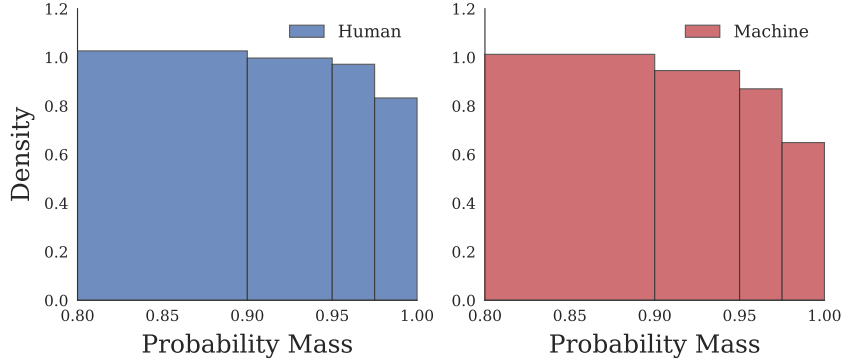


Figure 4: DMAP plots of human-written and GPT-5.4-generated text from the Modern-Raid dataset focusing on the tail of the distribution (0.8, 1). This highlights the region of biggest difference between human and GPT-5.4 through the lens of the OPT-125m distribution.

All learned calibrators are trained for 50 epochs. We used the AdamW optimizer, a learning rate of $1e-3$, weight decay of $1e-4$, batch size of 4096 and dropout 0.1, all of which are defaults.

95% confidence intervals are computed using bootstrap resampling with 10000 iterations.

Local DMAP predictor. For local-DMAP defined in Appendix C, we train a two-layer MLP with input dimension 30 and hidden dimension 64, with GELU activations and dropout between layers. The output layer has dimension 64×6 ; applying softmax yields a predicted distribution over the six bins of the DMAP histogram. The network is trained using soft cross-entropy between predicted and target distributions.

Local Gaussian predictors. For scalar score functions such as log-likelihood and log-rank, we learn a local Gaussian predictor of $g(x_i|Z(x_i), H)$ and $g(x_i|Z(x_i), M)$ separately. The architecture follows that of the local DMAP predictor, with the output layer replaced by one of dimension 64×2 producing a pair (μ, σ) . We take μ directly and apply softplus to σ to ensure non-negativity. These networks are trained using negative log-likelihood.

Detector model. In all experiments we use OPT-125M as the detector language model, which may easily be run on consumer hardware. The exception is the Binoculars baseline, which requires a scorer-observer model pair. For Binoculars we follow the original experimental setup of [4], using Falcon-3-7B and Falcon-3-7B-Instruct. For DALD, we use opt-125m as the base model and fine tune it using the recipe from [6] exactly, using the same training set for DALD that we use for calibrating other detectors.

Training and evaluation protocol. For each dataset and generator, we hold out a fixed subset of human-written and machine-generated texts for training local predictors. Specifically, we reserve 500 human-written and 500 machine-generated texts per generator for calibration training, with the remainder used for evaluation. We report AUROC as our primary metric, which does not require a fixed threshold and allows comparison across datasets and generators.

D.1 Datasets

Classic RAID. The RAID dataset [14] contains human-written texts across eight domains together with machine-generated counterparts produced by a variety of models available in 2024. We retain the human texts and those generated by ChatGPT 3.5 and GPT-4, as we are interested in outputs of instruction-tuned models. We use texts generated by pure sampling without repetition penalty or evasion attacks. Each entry includes a title field; models are prompted according to domain, for example in the recipes domain the prompt is: Write a recipe for "title". For this dataset we have 5994 texts in the train split and 34, 119 texts in the test split.

Table 4: Companion to Table 1 with 95% confidence intervals.

Method	Modern RAID			Peer-Review		
	GPT-5.4	Gemini	Claude	GPT-4o	Gemini	Claude
Baseline Log-Surprisal	(0.554–0.570)	(0.498–0.513)	(0.624–0.638)	(0.625–0.646)	(0.548–0.570)	(0.504–0.525)
Calibrated Log-Surprisal	(0.915–0.922)	(0.889–0.897)	(0.934–0.940)	(0.951–0.958)	(0.966–0.971)	(0.988–0.991)
Baseline Log-Rank	(0.536–0.552)	(0.461–0.476)	(0.601–0.616)	(0.592–0.613)	(0.516–0.538)	(0.469–0.490)
Calibrated Log-Rank	(0.851–0.861)	(0.775–0.787)	(0.864–0.874)	(0.818–0.834)	(0.827–0.842)	(0.905–0.916)
Baseline Token-NPR	(0.595–0.610)	(0.679–0.692)	(0.762–0.774)	(0.606–0.626)	(0.574–0.595)	(0.527–0.548)
Calibrated Token-NPR	(0.829–0.840)	(0.743–0.755)	(0.851–0.861)	(0.801–0.817)	(0.805–0.821)	(0.894–0.906)
Baseline Token-FastDetect	(0.620–0.635)	(0.728–0.741)	(0.794–0.805)	(0.630–0.650)	(0.596–0.617)	(0.535–0.556)
Calibrated Token-FastDetect	(0.849–0.859)	(0.800–0.811)	(0.863–0.873)	(0.855–0.869)	(0.854–0.868)	(0.927–0.937)
Baseline DMAP	(0.682–0.696)	(0.773–0.785)	(0.800–0.811)	(0.826–0.841)	(0.949–0.956)	(0.855–0.868)
Calibrated DMAP	(0.936–0.942)	(0.934–0.940)	(0.959–0.963)	(0.971–0.976)	(0.977–0.981)	(0.993–0.995)

Table 5: Companion to Table 2 with 95% confidence intervals.

Method	Modern RAID			Peer-Review		
	GPT-5.4	Gemini	Claude	GPT-4o	Gemini	Claude
NPR	(0.519–0.533)	(0.496–0.510)	(0.547–0.561)	(0.591–0.608)	(0.573–0.591)	(0.487–0.505)
Binoculars	(0.685–0.699)	(0.529–0.545)	(0.621–0.636)	(0.280–0.298)	(0.615–0.636)	(0.497–0.519)
Fast-DetectGPT	(0.622–0.636)	(0.726–0.739)	(0.794–0.805)	(0.630–0.650)	(0.596–0.617)	(0.533–0.554)
DALD	(0.890–0.899)	(0.954–0.959)	(0.940–0.946)	(0.845–0.859)	(0.858–0.871)	(0.961–0.968)
Calibrated DMAP	(0.936–0.942)	(0.934–0.940)	(0.959–0.963)	(0.971–0.976)	(0.977–0.981)	(0.993–0.995)

Modern RAID. To evaluate on outputs of current frontier models, we regenerate responses following the RAID prompt templates exactly, using GPT-5.4 [9], Gemini 3.1 Pro [10], and Claude Sonnet 4.6 [11] as generators. We use default settings for all generators; for Gemini this includes top-p=0.95. We have 7980 texts in the train split and 45,396 in the test split.

Peer-review benchmark. Our third dataset is the machine-generated peer-review benchmark of [18]. Models are presented with papers submitted to ICLR 2021–2022 or NeurIPS 2021–2022, together with conference-specific guidelines and review templates, and asked to produce a review. We consider only texts generated by instruction-tuned models: GPT-4o, Claude Sonnet 3.5, and Gemini Pro 1.5. Conference-specific formatting is removed and only the main text of each review is retained. We have 8198 texts in the train split and 22164 texts in the test split.

Text length. Our main results analyse detector performance when given only the first 200 tokens of each text. This controlled-length setting facilitates direct comparison across datasets and generators, and ensures that baseline detector scores are not confounded by text length effects whose expected value may vary with token count.

D.2 Reproducing Figure 2.

The upper plots are 2D TSNE projections [19] of the OPT-125m embeddings of a single text (human/gpt5 generated) with TSNE perplexity 20. To smooth the plot local averages on a 12x12 grid and computed and the surface generated using a cubic interpolation. The text is from the poetry domain of Modern RAID. The lower plots simply visualize a heatmap over 2,000 texts from RAID (Human and GPT-5.4 generated) of the log probability across 50 clusters obtained via k-means on the hidden space.

E Further Results

E.1 Confidence Intervals

This section presents companion tables to Table 1 and Table 2 containing 95% confidence intervals for each value obtained via bootstrap resampling from our test set with 10000 iterations.

Table 6: Human vs. AI Detection Performance on Classic RAID dataset on 200 tokens (Key Metrics). Values are mean (95% confidence interval).

Model	Method	TPR@0.1%	TPR@1%	AUROC
ChatGPT	Baseline log-surprisal	3.04 (0.01–9.42)	18.70 (17.39–20.16)	0.8519 (0.8470–0.8567)
	Baseline log-rank	3.51 (1.20–10.09)	19.62 (18.21–22.16)	0.8396 (0.8344–0.8446)
	Baseline Fast-DetectGPT	37.70 (33.04–43.11)	65.70 (63.61–68.45)	0.9642 (0.9621–0.9663)
	Token Fast-Detect	32.58 (22.19–39.72)	69.16 (66.27–71.23)	0.9666 (0.9645–0.9686)
	Token NPR	25.31 (15.91–37.81)	64.14 (61.65–66.46)	0.9602 (0.9579–0.9625)
	Baseline NPR	0.52 (0.31–0.71)	5.06 (4.28–5.82)	0.7053 (0.6990–0.7116)
	Baseline Binoculars	20.08 (15.26–25.49)	43.83 (40.57–46.21)	0.8933 (0.8892–0.8976)
	DMAP	47.54 (40.90–55.65)	79.06 (76.92–80.89)	0.9824 (0.9809–0.9838)
	DALD	70.77 (66.27–77.35)	89.20 (87.14–90.74)	0.9917 (0.9905–0.9929)
	Calibrated Log-Surprisal	47.31 (37.96–59.78)	79.96 (78.17–82.03)	0.9852 (0.9839–0.9865)
	Calibrated Log-Rank	0.99 (0.05–24.52)	62.17 (60.27–64.41)	0.9412 (0.9379–0.9445)
	Calibrated Token Fast-Detect	23.73 (3.24–33.68)	63.94 (61.99–66.25)	0.9491 (0.9460–0.9519)
	Calibrated Token NPR	0.18 (0.05–0.26)	61.07 (56.55–63.73)	0.9243 (0.9206–0.9279)
	Calibrated DMAP	67.62 (65.16–74.43)	88.66 (87.60–90.36)	0.9910 (0.9900–0.9919)
GPT-4	Baseline log-surprisal	1.18 (0.00–5.21)	10.91 (10.14–11.71)	0.6342 (0.6269–0.6413)
	Baseline log-rank	1.41 (0.37–5.73)	10.65 (9.93–11.70)	0.6151 (0.6076–0.6223)
	Baseline Fast-DetectGPT	4.90 (3.70–6.47)	16.04 (14.66–17.91)	0.7859 (0.7801–0.7917)
	Token Fast-Detect	2.66 (1.23–4.06)	15.78 (14.03–17.39)	0.7867 (0.7809–0.7925)
	Token NPR	1.74 (0.44–4.07)	15.02 (13.49–16.52)	0.7696 (0.7635–0.7756)
	Baseline NPR	0.16 (0.07–0.25)	1.91 (1.55–2.27)	0.5767 (0.5699–0.5835)
	Baseline Binoculars	1.13 (0.55–1.64)	5.57 (4.56–6.51)	0.6319 (0.6247–0.6392)
	DMAP	1.91 (1.17–3.10)	13.29 (11.89–14.95)	0.8238 (0.8183–0.8291)
	DALD	20.62 (17.43–25.69)	41.89 (38.71–44.26)	0.9372 (0.9338–0.9405)
	Calibrated Log-Surprisal	13.40 (8.55–15.36)	32.93 (29.71–35.48)	0.9023 (0.8985–0.9062)
	Calibrated Log-Rank	0.20 (0.09–1.05)	20.24 (18.30–22.12)	0.8145 (0.8091–0.8200)
	Calibrated Token Fast-Detect	0.82 (0.49–6.20)	21.56 (18.83–23.32)	0.8290 (0.8238–0.8342)
	Calibrated Token NPR	0.18 (0.07–0.33)	13.76 (11.69–16.28)	0.7905 (0.7847–0.7963)
	Calibrated DMAP	30.79 (22.90–34.72)	51.55 (48.80–54.68)	0.9414 (0.9385–0.9443)

E.2 Classic Raid Results

We present in Table 6 the table of results on the classic RAID dataset. This contains text generated by older models and is mainly used for performance comparison with more modern models.

E.3 Full Results for Modern Raid and Peer-Review

We include in Tables 7 and 8 results summarized in the main text.

E.4 Multi-generator detection

Table 9 reports results on the more challenging setting where texts from multiple generators are pooled and the task is to classify AI-generated versus human-written text. Calibration continues to improve performance over all uncalibrated baselines, demonstrating that the local calibration step is effective even when the training distribution spans multiple generators.

E.5 Domain-shift experiments

Table 10 summarizes detection performance under topic shift using a leave-one-domain-out protocol on Modern RAID. Across generators and methods, moving from in-domain to out-of-domain evaluation results in a noticeable degradation in performance, with AUROC typically dropping by around 8–12 percentage points. This behavior is consistent with the core observation of the paper that the local likelihood-based signal is not uniform across topics. While this effect is notable, locally calibrated likelihood methods remain substantially more effective than their uncalibrated alternatives. In particular, even imperfect local calibration mitigates the impact of domain shift relative to uncalibrated aggregation, confirming that poor calibration is still preferable to none.

Table 7: Human vs. AI Detection Performance (Key Metrics) on Modern RAID dataset on 200 tokens. Values are mean (95% confidence interval).

Model	Method	TPR@0.1%	TPR@1%	AUROC
GPT-5	Baseline Log-Surprisal	0.74 (0.01–1.73)	5.65 (4.93–6.43)	0.5617 (0.5541–0.5695)
	Baseline Log-Rank	0.55 (0.09–1.48)	4.93 (4.17–6.19)	0.5440 (0.5364–0.5519)
	Fast-DetectGPT Baseline	1.30 (0.90–2.08)	8.40 (7.18–9.86)	0.6290 (0.6217–0.6364)
	Token Fast-Detect	0.66 (0.16–1.13)	7.86 (6.27–8.98)	0.6275 (0.6202–0.6350)
	Token NPR	0.90 (0.20–1.33)	7.87 (6.88–8.96)	0.6025 (0.5950–0.6101)
	Baseline NPR	0.10 (0.03–0.19)	1.67 (1.35–2.04)	0.5259 (0.5190–0.5328)
	Baseline Binoculars	1.75 (1.30–2.83)	10.53 (9.29–11.59)	0.6920 (0.6853–0.6989)
	DMAP	0.85 (0.48–1.52)	6.75 (5.55–7.55)	0.6891 (0.6821–0.6960)
	DALD	30.22 (27.71–33.67)	42.70 (40.65–45.50)	0.8943 (0.8898–0.8988)
	Calibrated Log-Surprisal	7.33 (4.81–9.23)	32.95 (29.07–36.30)	0.9182 (0.9146–0.9218)
	Calibrated Log-Rank	2.73 (0.86–6.95)	25.92 (23.11–28.09)	0.8559 (0.8508–0.8608)
	Calibrated Token Fast-Detect	3.74 (2.17–5.20)	19.31 (16.08–22.06)	0.8538 (0.8488–0.8589)
	Calibrated Token NPR	2.02 (0.34–3.92)	16.58 (14.89–18.52)	0.8342 (0.8288–0.8395)
Calibrated DMAP	29.14 (19.76–34.94)	54.95 (52.83–57.48)	0.9388 (0.9358–0.9417)	
Gemini	Baseline Log-Surprisal	0.02 (0.00–0.04)	0.11 (0.05–0.19)	0.5057 (0.4982–0.5132)
	Baseline Log-Rank	0.02 (0.00–0.04)	0.06 (0.02–0.12)	0.4683 (0.4609–0.4759)
	Fast-DetectGPT Baseline	0.19 (0.10–0.40)	2.85 (2.28–3.72)	0.7329 (0.7263–0.7393)
	Token Fast-Detect	0.15 (0.04–0.31)	3.10 (2.35–3.83)	0.7344 (0.7279–0.7408)
	Token NPR	0.36 (0.05–0.58)	3.52 (2.88–4.23)	0.6856 (0.6787–0.6924)
	Baseline NPR	0.07 (0.02–0.14)	0.91 (0.72–1.18)	0.5031 (0.4961–0.5100)
	Baseline Binoculars	0.38 (0.22–0.72)	3.32 (2.80–3.84)	0.5369 (0.5294–0.5445)
	DMAP	0.07 (0.02–0.27)	1.59 (1.22–2.17)	0.7791 (0.7731–0.7851)
	DALD	34.74 (29.39–38.76)	56.44 (53.58–59.52)	0.9568 (0.9541–0.9593)
	Calibrated Log-Surprisal	14.03 (10.92–18.46)	34.73 (32.84–37.89)	0.8927 (0.8886–0.8968)
	Calibrated Log-Rank	0.56 (0.14–1.69)	11.58 (10.58–12.80)	0.7809 (0.7750–0.7868)
	Calibrated Token Fast-Detect	4.33 (2.37–7.27)	15.60 (14.47–17.57)	0.8052 (0.7995–0.8108)
	Calibrated Token NPR	0.22 (0.10–0.94)	10.55 (9.44–11.64)	0.7488 (0.7425–0.7551)
Calibrated DMAP	23.13 (20.54–35.51)	52.21 (49.56–54.71)	0.9368 (0.9338–0.9398)	
Claude	Baseline Log-Surprisal	0.06 (0.00–0.20)	2.17 (1.71–2.83)	0.6309 (0.6237–0.6381)
	Baseline Log-Rank	0.04 (0.00–0.15)	1.63 (1.23–2.49)	0.6083 (0.6010–0.6156)
	Fast-DetectGPT Baseline	2.21 (1.53–3.63)	13.44 (11.81–15.58)	0.7993 (0.7937–0.8050)
	Token Fast-Detect	1.43 (0.49–2.27)	13.27 (10.97–14.59)	0.7996 (0.7939–0.8052)
	Token NPR	1.90 (0.52–2.65)	12.49 (11.21–13.78)	0.7680 (0.7621–0.7741)
	Baseline NPR	0.21 (0.07–0.33)	1.80 (1.45–2.16)	0.5541 (0.5472–0.5609)
	Baseline Binoculars	1.58 (1.12–2.61)	9.06 (7.85–9.95)	0.6283 (0.6213–0.6357)
	DMAP	0.84 (0.42–1.83)	7.35 (6.35–9.12)	0.8052 (0.7996–0.8107)
	DALD	26.97 (20.53–31.32)	48.49 (45.62–50.90)	0.9428 (0.9397–0.9458)
	Calibrated Log-Surprisal	8.83 (2.67–18.67)	49.47 (45.95–52.20)	0.9369 (0.9338–0.9399)
	Calibrated Log-Rank	0.04 (0.01–4.44)	29.74 (26.47–33.07)	0.8691 (0.8643–0.8740)
	Calibrated Token Fast-Detect	2.33 (0.03–4.61)	32.67 (30.05–35.80)	0.8682 (0.8634–0.8730)
	Calibrated Token NPR	0.05 (0.01–0.43)	24.50 (21.40–27.92)	0.8559 (0.8509–0.8610)
Calibrated DMAP	37.34 (31.57–41.38)	63.50 (61.60–66.20)	0.9612 (0.9590–0.9634)	

F Examining the Gaussian Assumption of our Calibration Step

Our calibration step for log-surprisal, log-rank, Fast-DetectGPT and NPR is based on learning Gaussian predictors. More precisely, for each score function (such as log surprisal), generator (such as GPT-5.4 or human) and feature vector (30-dimensional vector containing information on where the context sits in hidden space and what the five largest predicted next-token probabilities are given context) we predict a pair (μ, σ) such that the corresponding Gaussian models the distribution of score functions for texts from the given generator in contexts with the given feature vector. We used this Gaussian assumption in the implementation of our calibration step as part of our philosophy of implementing the simplest experiments possible in order to demonstrate the correctness of our central idea, that adding the calibration step substantially lifts the performance of detectors. In Section 6 we mentioned that this Gaussian assumption was likely suboptimal, and that a more advanced local model of the distributions would likely lead to performance uplift.

Here we examine the under-performance of our Gaussian assumption for log-surprisal of GPT-5.4 text. Given a predicted local Gaussian with parameters (μ, σ) and a value $g(w_i)$ of the score of

Table 8: Human vs. AI Detection Performance on the Peer-Review Dataset (Key Metrics). Values are mean (95% confidence interval).

Model	Method	TPR@0.1%	TPR@1%	AUROC
GPT-4o	Baseline Log-Surprisal	0.00 (0.00–0.00)	0.52 (0.11–0.94)	0.6354 (0.6251–0.6456)
	Baseline Log-Rank	0.00 (0.00–0.04)	0.32 (0.11–0.83)	0.6021 (0.5917–0.6125)
	Baseline Fast-DetectGPT	0.14 (0.04–0.58)	2.06 (1.57–2.66)	0.6397 (0.6296–0.6498)
	Token Fast-Detect	0.13 (0.04–0.56)	1.97 (1.51–2.64)	0.6403 (0.6303–0.6504)
	Token NPR	0.13 (0.04–0.41)	1.80 (1.37–2.34)	0.6157 (0.6056–0.6259)
	Baseline NPR	0.16 (0.01–0.37)	1.82 (1.18–2.32)	0.5996 (0.5907–0.6083)
	Baseline Binoculars	0.02 (0.00–0.07)	0.31 (0.16–0.50)	0.2887 (0.2795–0.2982)
	DMAP	0.49 (0.18–1.04)	7.95 (6.28–10.17)	0.8337 (0.8262–0.8411)
	DALD	8.51 (3.80–12.93)	27.42 (24.03–30.55)	0.8523 (0.8453–0.8593)
	Calibrated Log-Surprisal	32.71 (17.33–43.59)	64.35 (60.86–66.76)	0.9544 (0.9508–0.9580)
	Calibrated Log-Rank	0.22 (0.02–1.23)	13.72 (10.78–17.97)	0.8262 (0.8182–0.8340)
	Calibrated Token Fast-Detect	1.48 (0.27–6.68)	24.35 (19.87–29.50)	0.8623 (0.8552–0.8693)
	Calibrated Token NPR	1.21 (0.34–3.56)	14.84 (12.43–18.04)	0.8089 (0.8007–0.8172)
	Calibrated DMAP	33.04 (27.94–42.72)	63.43 (57.86–66.33)	0.9734 (0.9709–0.9758)
Gemini	Baseline Log-Surprisal	0.00 (0.00–0.00)	0.29 (0.07–0.62)	0.5590 (0.5483–0.5698)
	Baseline Log-Rank	0.00 (0.00–0.02)	0.25 (0.09–0.61)	0.5269 (0.5162–0.5377)
	Baseline Fast-DetectGPT	0.23 (0.07–0.61)	1.89 (1.35–2.50)	0.6063 (0.5958–0.6168)
	Token Fast-Detect	0.22 (0.07–0.59)	1.86 (1.29–2.52)	0.6067 (0.5962–0.6172)
	Token NPR	0.18 (0.05–0.38)	1.52 (1.07–2.04)	0.5843 (0.5737–0.5950)
	Baseline NPR	0.11 (0.00–0.29)	1.28 (0.79–1.75)	0.5816 (0.5725–0.5906)
	Baseline Binoculars	0.74 (0.36–1.36)	4.04 (3.13–5.49)	0.6255 (0.6152–0.6358)
	DMAP	5.76 (4.45–9.94)	37.81 (31.73–43.03)	0.9523 (0.9486–0.9559)
	DALD	12.08 (6.51–19.41)	33.75 (30.40–38.79)	0.8646 (0.8577–0.8712)
	Calibrated Log-Surprisal	38.08 (26.44–41.23)	67.73 (63.40–70.19)	0.9686 (0.9658–0.9713)
	Calibrated Log-Rank	0.92 (0.38–2.82)	18.50 (16.39–23.43)	0.8346 (0.8271–0.8421)
	Calibrated Token Fast-Detect	2.73 (1.68–7.50)	24.40 (21.13–29.10)	0.8609 (0.8540–0.8678)
	Calibrated Token NPR	0.81 (0.31–2.49)	15.30 (12.13–18.67)	0.8129 (0.8050–0.8209)
	Calibrated DMAP	43.96 (34.31–55.98)	71.25 (67.99–74.15)	0.9788 (0.9767–0.9808)
Claude	Baseline Log-Surprisal	0.00 (0.00–0.00)	0.02 (0.00–0.16)	0.5144 (0.5036–0.5250)
	Baseline Log-Rank	0.00 (0.00–0.00)	0.05 (0.00–0.25)	0.4791 (0.4685–0.4897)
	Baseline Fast-DetectGPT	0.04 (0.00–0.18)	0.56 (0.36–0.87)	0.5433 (0.5327–0.5538)
	Token Fast-Detect	0.02 (0.00–0.16)	0.60 (0.36–0.87)	0.5453 (0.5346–0.5558)
	Token NPR	0.07 (0.00–0.18)	0.63 (0.40–0.97)	0.5372 (0.5265–0.5476)
	Baseline NPR	0.11 (0.00–0.33)	0.96 (0.70–1.35)	0.4958 (0.4867–0.5051)
	Baseline Binoculars	0.25 (0.11–0.51)	1.66 (1.20–2.27)	0.5077 (0.4968–0.5186)
	DMAP	0.87 (0.50–2.29)	13.52 (10.96–15.70)	0.8613 (0.8545–0.8680)
	DALD	38.11 (29.86–46.34)	68.19 (65.15–70.97)	0.9646 (0.9613–0.9677)
	Calibrated Log-Surprisal	59.15 (41.64–69.42)	83.86 (81.62–86.33)	0.9897 (0.9882–0.9910)
	Calibrated Log-Rank	3.74 (1.60–8.06)	26.59 (21.95–36.89)	0.9104 (0.9047–0.9161)
	Calibrated Token Fast-Detect	11.02 (9.45–23.06)	46.25 (42.11–51.55)	0.9322 (0.9271–0.9371)
	Calibrated Token NPR	7.48 (2.67–13.33)	31.01 (25.28–35.36)	0.8996 (0.8937–0.9055)
	Calibrated DMAP	64.02 (57.15–71.36)	88.60 (84.46–91.00)	0.9943 (0.9933–0.9951)

Table 9: Performance of Calibrated DMAP and baselines at distinguishing AI vs human text. For each dataset we combine human text together with AI generated text from all three models and evaluate the effectiveness of Calibrated DMAP at distinguishing between AI and human. While the performance of Calibrated DMAP drops significantly compared to the case when it is targeting one known generator, it still outperforms baselines.

Method	Peer-Review			Modern RAID		
	TPR@0.1%	TPR@1%	AUROC	TPR@0.1%	TPR@1%	AUROC
Binoculars Baseline	1.96	9.08	0.5617	0.73	5.88	0.5677
Fast-DetectGPT Baseline	6.46	20.76	0.8040	6.68	16.82	0.7418
Calibrated DMAP	67.36	92.56	0.9967	2.79	22.51	0.9043
Log-Likelihood Baseline	0.00	2.44	0.7891	0.01	5.54	0.5892
Log-Rank Baseline	0.00	2.44	0.7643	0.02	4.76	0.5664
DALD	13.60	36.27	0.8733	28.44	45.71	0.9240

Table 10: In-domain (ID) vs. out-of-domain (OOD) detection performance under topic shift on Modern RAID. Experiments follow a leave-one-domain-out protocol over eight domains: models are trained on samples from 7/8 domains. OOD performance is evaluated on test samples from the held-out domain, while ID performance is evaluated on test samples drawn from the same 7/8 training domains. Each entry reports the mean \pm standard deviation over all domain splits.

Method	Generator	ID AUROC	OOD AUROC	ID TPR@1%	OOD TPR@1%
Local DMAP	GPT-5	0.9459 \pm 0.0097	0.8403 \pm 0.0705	46.83 \pm 8.10	16.72 \pm 16.07
	Gemini	0.9358 \pm 0.0116	0.8504 \pm 0.0655	31.94 \pm 7.69	12.20 \pm 14.26
	Claude	0.9547 \pm 0.0110	0.8719 \pm 0.0883	50.73 \pm 9.26	20.23 \pm 23.69
Local Log-Surprisal	GPT-5	0.9574 \pm 0.0111	0.8383 \pm 0.1458	50.03 \pm 10.11	27.32 \pm 28.82
	Gemini	0.9072 \pm 0.0217	0.8562 \pm 0.0634	17.60 \pm 9.14	5.58 \pm 3.88
	Claude	0.9359 \pm 0.0173	0.8419 \pm 0.1265	41.43 \pm 10.38	25.28 \pm 38.47
Local Log-Rank	GPT-5	0.9209 \pm 0.0107	0.8382 \pm 0.0679	31.15 \pm 7.93	22.54 \pm 16.31
	Gemini	0.8624 \pm 0.0185	0.7614 \pm 0.0795	15.60 \pm 6.29	3.43 \pm 2.62
	Claude	0.9060 \pm 0.0120	0.8188 \pm 0.0815	36.75 \pm 7.55	14.45 \pm 19.34
Local Fast-Detect	GPT-5	0.9038 \pm 0.0106	0.8065 \pm 0.1184	16.81 \pm 11.14	21.70 \pm 21.46
	Gemini	0.8620 \pm 0.0076	0.7634 \pm 0.0963	12.84 \pm 3.70	3.46 \pm 2.61
	Claude	0.9228 \pm 0.0107	0.8081 \pm 0.1053	38.72 \pm 6.87	16.13 \pm 22.90
Local NPR	GPT-5	0.8931 \pm 0.0093	0.7994 \pm 0.0874	20.88 \pm 6.89	19.23 \pm 17.52
	Gemini	0.8415 \pm 0.0122	0.7385 \pm 0.0868	15.16 \pm 3.86	3.65 \pm 3.99
	Claude	0.9049 \pm 0.0122	0.8259 \pm 0.0761	39.31 \pm 5.83	17.56 \pm 18.88

the true next token, we plot the Z-score $\frac{g(w_i) - \mu}{\sigma}$. We run this over all of the texts in the test set, a little over five million tokens in total and plot our results in Figure 5. If the Gaussian distributions matched the underlying data well, the resulting plot of Z-scores would be distributed according to $\mathcal{N}(0, 1)$. We stress that this plot is not assessing the efficacy of individual Gaussian predictors, rather, we aggregate over the test set to see whether there are systematic failures of the local Gaussians to model the underlying data. The clear skew in the histogram, together with the fact that tails are not symmetric, shows that there is clear room for improvement in picking a calibration model.

G Degradation of Detector Performance Over Time

Our results show clearly that the performance of state-of-the-art detectors at distinguishing human text from that generated by instruction-tuned models is getting worse with more modern models. This is best seen by comparing classic and modern RAID (Tables 7 and 6). Across our baseline detectors designed to extract the likelihood signal, there is degradation in performance as one goes from GPT-3.5 and GPT-4 in the classic RAID dataset to the models of the modern RAID dataset.

H Optimizing DMAP

Table 11 reports results from a small hyperparameter sweep designed to assess how much headroom remains beyond the minimally tuned configurations used in the main paper. The baseline results intentionally reflect a near-default setup and were chosen to isolate the effect of local calibration itself across multiple detectors rather than to optimize absolute performance. This section shows that modest optimization of the calibration step yields stronger performance across all generators. We first increase the capacity of the calibration model (raising the hidden dimension of the two-layer MLP from 64 to 256), and then increase the number of DMAP bins to capture finer-grained distributional structure. Together, these changes better match the expressivity of the calibration step to the available training data. Finally, we increase the number of training epochs to ensure convergence.

Under both full-context and 200-token evaluation, the optimized DMAP consistently outperforms competing detectors at all reported thresholds, achieving the highest TPR@1% and AUROC for GPT-5, Gemini, and Claude on the Modern RAID dataset. This demonstrates that the gains reported in the main text are conservative, and that local calibration not only provides a principled correction to likelihood aggregation, but also supports substantially stronger detector variants once modest hyperparameter tuning is applied.

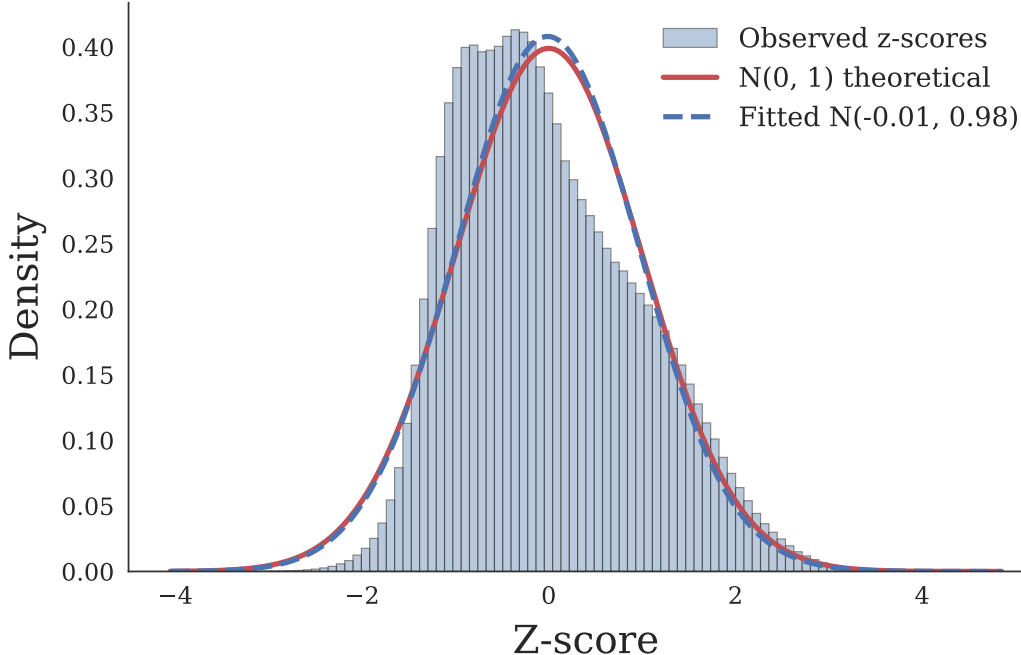


Figure 5: Z-scores of log-surprisal of GPT-5.4 generated text relative to learned calibrating Gaussians. The fact that our observed Z-scores are not well aligned with $\mathcal{N}(0, 1)$ shows a systematic issue with the Gaussian assumption in the local-calibration step, using a more expressive family of distributions for the local calibration is expected to substantially lift performance of our calibrated detectors.

Table 11: Hyperparameter sweep results for full-context vs. 200-token variants.

Setting	Context	GPT-5		Gemini		Claude	
		TPR@1%	AUROC	TPR@1%	AUROC	TPR@1%	AUROC
Baseline	Full	68.52%	0.9649	59.65	0.9640	70.88	0.9763
	200 tokens	54.95%	0.9388	52.21	0.9368	63.50	0.9612
Increase capacity [64 → 256]	Full	73.02% (+4.50)	0.9747 (+0.010)	67.15% (+7.50)	0.9720 (+0.008)	77.96% (+7.08)	0.9816 (+0.005)
	200 tokens	59.35% (+4.40)	0.9513 (+0.013)	55.40% (+3.19)	0.9461 (+0.009)	69.11% (+5.61)	0.9679 (+0.007)
Increase num bins [6 → 12]	Full	81.19% (+12.67)	0.9828 (+0.018)	72.37% (+12.72)	0.9742 (+0.010)	82.14% (+11.26)	0.9857 (+0.009)
	200 tokens	67.08% (+12.13)	0.9665 (+0.028)	62.99% (+10.78)	0.9520 (+0.015)	73.02% (+9.52)	0.9745 (+0.013)
Increase num epochs [50 → 150]	Full	81.10% (+12.58)	0.9840 (+0.019)	74.53% (+14.88)	0.9769 (+0.013)	83.61% (+12.73)	0.9871 (+0.011)
	200 tokens	70.00% (+15.05)	0.9675 (+0.029)	65.26% (+13.05)	0.9576 (+0.021)	74.17% (+10.67)	0.9768 (+0.016)

I A comparison with DALD

In this section we discuss how our approach differs from DALD [6]. The purpose of DALD is to fine-tune the detector model on generator-model outputs so as to bring the black-box performance of Fast-DetectGPT in line with the white-box performance (where the generator model and detector model are the same). This is well-motivated, there is a clear drop off in performance of Fast-DetectGPT between the white-box and black-box cases, and the results of DALD are impressive.

On the surface, there is some similarity between our method and that of DALD, we are both motivated to use outputs of a particular generator model to improve the performance of our detector model. However the fundamental logic of DALD continues to globally average token-level likelihood signals, specifically they use Fast-DetectGPT with their fine-tuned detector. This ignores the local structure which our calibrated detectors seek to use.

One advantage that DALD has is that very little design choice is required, it can use off-the-shelf fine-tuning algorithms and the well-studied Fast-DetectGPT approach. By contrast, our calibration step does require design choices: how long to run for, how large the hidden dimension of the calibration head should be, how many PCA dimensions we should have, and what type of distribution to impose on the local calibration step. Furthermore, the theoretical justification for our method relies on the

idea that we have reasonable proxies for the true probabilities of a given token score, given features and generator.

J Capping text-length

We note an issue with the way Fast-DetectGPT (and hence DALD) deals with texts of different lengths. This was previously pointed out in [8]. While the issue is not very easy to see directly from the paper, reading the function `get_sampling_discrepancy_analytic` from the GitHub repository makes the issue clear.

While most of our detectors average a token level score function g , Fast-DetectGPT returns $\frac{\sum_{i=1}^n g(x_i)}{\sigma}$. The denominator σ is obtained by taking the square root of the sum of token-level variances. These token-level variances grow roughly linearly, or slightly faster once one accounts for covariance. Thus the denominator should grow a little faster than \sqrt{n} , while the numerator may be expected to grow linearly in n . This introduces a bias when evaluating human vs machine text where the typical length of machine and human text is different. This bias is one of the motivating reasons that all texts are capped to 200 tokens in our main results table.

K Computation Time

We report the time taken for a complete experimental run on the Peer-review dataset, which consists of 8,198 training texts (split between human, GPT-4o, Claude, and Gemini) and 22,164 test texts. All experiments requiring GPU acceleration were run on a single NVIDIA A100.

Table 12: Computation time breakdown for a complete run on the Peer-review dataset.

Stage	Hardware	Time
<i>Feature extraction and calibration</i>		
PCA fitting	GPU	6 min
Feature extraction (training set)	GPU	8 min
Feature extraction (test set)	GPU	24 min
Local calibration training (20 runs)	GPU	70 min
<i>Baselines</i>		
Binoculars (200 tokens)	GPU	3.5 hrs
Binoculars (full texts)	GPU	8.1 hrs
NPR (200 tokens)	GPU	14 hrs
Fast-DetectGPT (200 tokens)	GPU	12 min
<i>Other</i>		
Bootstrap CIs & miscellaneous	CPU	6 hrs
Total (Peer-review)	GPU / CPU	27h 40m / 6h

The total runtime is dominated by the NPR and Binoculars baselines, which require expensive forward passes through large language models. Our calibration approach adds minimal overhead: feature extraction and calibration training together require under two hours of GPU time.

Across all three datasets, including preliminary experiments, debugging, and reruns due to data errors, total experimental compute was approximately 220 GPU-hours and 15 CPU-hours.